

LETTERS

https://doi.org/10.1070/QEL17382

Smart adaptive optical system for correcting the laser wavefront distorted by atmospheric turbulence

A.L. Rukosuev, V.N. Belousov, A.N. Nikitin, Yu.V. Sheldakova, A.V. Kudryashov, V.A. Bogachev, M.V. Volkov, S.G. Garanin, F.A. Starikov

Abstract. **An adaptive optical system is developed to correct the wavefront of laser radiation distorted by a turbulent air flow. The use of a field-programmable gate array as the main control element makes it possible to achieve a system bandwidth of 2 kHz. The results of experiments on dynamic correction of the phase of a laser beam distorted by a flow of heated air are presented and analysed.**

Keywords: *adaptive optics, wavefront sensor, field-programmable gate array, atmospheric turbulence.*

Compensation for the effect of a turbulent atmosphere on laser radiation is very important in solving problems of energy transfer and laser communication (see, e.g., [1–4]). The impact of air flows causes dynamic distortions of the beam wavefront and reduces the focusing quality. To correct the wavefront of laser radiation in real time, a high-speed adaptive optical system (AOS) is required. The spectrum of atmospheric fluctuations reaches frequencies of ~100 Hz and more [5]; therefore, according to [6], the operating frequency range of the AOS should exceed 1 kHz. When controlling AOS by a computer, this rate cannot be provided due to delays in the operating system [7]. The aim of this work is to study the correction of fast phase fluctuations using a created AOS with a 2 kHz bandwidth, controlled by hardware based on a field-programmable gate array (FPGA).

The AOS is schematically shown in Fig. 1. Laser radiation ($\lambda = 632$ nm, flat-profile beam 50 mm in diameter) is incident on an adaptive mirror (AM) and then on a wavefront sensor (WFS) of the Shack–Hartmann type. A bimorph 31-element AM (optical aperture, 50 mm in diameter; electrode ring width, 8 mm; electrode stroke, 2 μm; and first resonance frequency, 8.3 kHz) efficiently corrects low-order aberrations, which usually arise due to turbulence. The parameters of the WFS based on a JetCam-19 camera [8] are as follows: dynamic range, $\pm 50\lambda$; rms deviation, $\lambda/120$; microlens focal length, 12 mm; number of subapertures, 20 × 20; aperture, 4.8 × 4.8 mm; and frequency, 4000 fps at a resolution of 480 × 480 pixels. Video information from the WFS camera via optical fibre at a rate of 40 Gbit s^{-1} enters the video capture card comprising an Arria V FPGA, which controls the AOS. The FPGA provides fast computation due to hardware implementation and parallel processing. A personal computer (PC) serves only to select the FPGA operation mode and collect information from the FPGA about the phase correction process. For an independent check of the correction quality, the laser beam spot is controlled in the far field by focusing with a long-focus lens on a Gig-E DMK23GM021 camera.

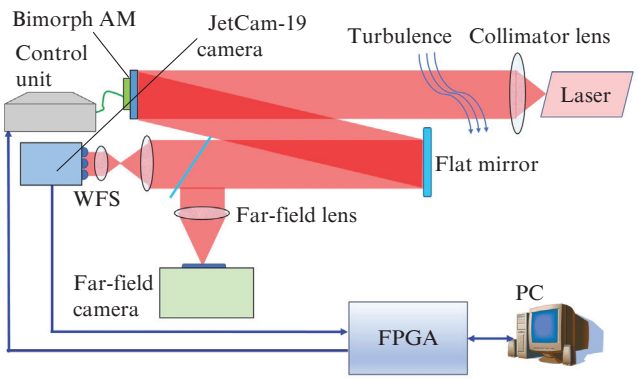

Figure 1. AOS schematic.

The FPGA processes video information and calculates control voltages, minimising the coordinate differences between the centres of mass (centroids) of spots in the corrected and reference beams on the hartmannogram of the WFS using the response functions of the AM. The FPGA uses the WFS camera interface at a low level and operates with image pixels in real time. Having obtained images of a part of the spots, the FPGA calculates the coordinates of the centroids and fills in the corresponding elements of the matrix to calculate the voltages. As a result, immediately after receiving the entire image by the FPGA, the calculated voltage vector is ready. The appropriate voltages are applied to the AM electrodes by the control unit, to which the FPGA also has a low-level access. The closed cycle time of the AOS is reduced to 0.5 ms, which corresponds to a bandwidth of 2 kHz. The timing diagram of one cycle of the AOS operation is presented in Fig. 2.

Experiments on the dynamic phase correction of laser beam distortions created by the heated air flow from a fan heater (see Fig. 1) have been carried out. The computational analysis of the dynamics of experimental hartmannograms using the differential method [9] showed that the coherence

A.L. Rukosuev, A.N. Nikitin, Yu.V. Sheldakova, A.V. Kudryashov Institute of Geosphere Dynamics, Russian Academy of Sciences, Leninsky prosp. 38/1, 119334 Moscow, Russia; e-mail: alru@nightn.ru;
V.N. Belousov Lyratech LCC, Malaya Tulskaya ul. 16, apt. IV, room 3, 115191 Moscow, Russia;
V.A. Bogachev, M.V. Volkov, S.G. Garanin, F.A. Starikov Institute of Laser Physics Research, Russian Federal Nuclear Centre – All-Russian Research Institute of Experimental Physics, prosp. Mira 37, 607190 Sarov, Nizhny Novgorod region, Russia

Received 9 June 2020
Kvantovaya Elektronika **50** (8) 707–709 (2020)
Translated by V.L. Derbov

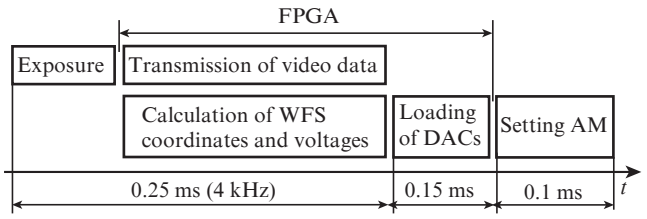

Figure 2. Timing diagram of one cycle of AOS operation.

radius of the turbulent path is ~1.5 cm, which is twice the size of the core electrode and six times the WFS subaperture with scaling taken into account. Since the aim of AOS is to keep the spots of the hartmannogram in reference positions in time, it is logical to draw conclusions about the time scale of turbulence, the influence of which is to be eliminated, from the dynamics of centroids. Figure 3 shows the time power spectrum of the centroid fluctuation in one of the central subapertures of the WFS (with statistically homogeneous turbulence, a similar picture is observed in each subaperture) and the dependence of the fraction of the spectral energy of fluctuations on frequency. It is noteworthy that in Fig. 3a, in the frequency range $\nu = 10-60$ Hz, a decrease in the spectral power according to the $\nu^{-5/3}$ law is observed, which is characteristic of the inertial interval of Kolmogorov atmospheric

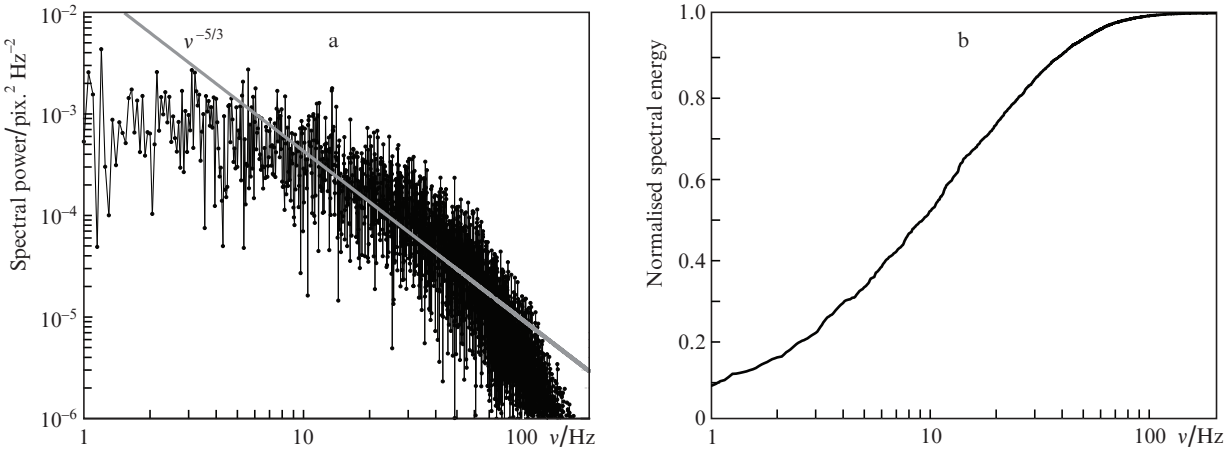

Figure 3. (a) Power spectrum of centroid fluctuations and (b) frequency dependence of the spectral energy fraction. The grey line shows the power dependence $\sim\nu^{-5/3}$.

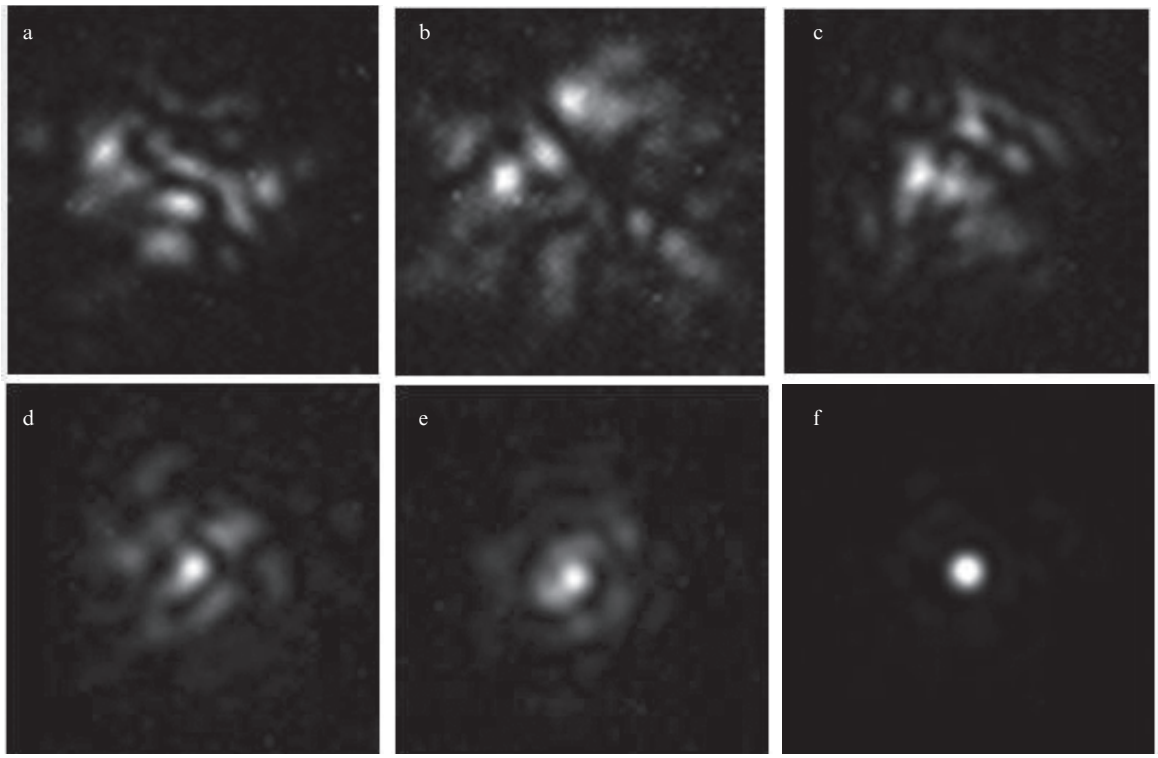

Figure 4. Typical instantaneous experimental distributions of laser radiation in the far field (a) in the absence of correction and (b–f) with correction with the frequency bandwidth ν_{AOS} = (b) 25, (c) 100, (d) 200, (e) 500, and (f) 1500 Hz.

turbulence [10]. Let us define the turbulence bandwidth ν_{turb} as the frequency within which 95% of the centroid fluctuation energy is contained. Then, according to Fig. 3b, we have $\nu_{turb} = 60$ Hz.

Figure 4 shows the characteristic instantaneous experimental distributions of laser radiation in the far field without adaptive phase correction and with correction for different AOS bandwidths ν_{AOS}. A decrease in ν_{AOS} was implemented by introducing a time delay after the end of the calculation of the control voltages for the AM (see Fig. 2), the exposure time remaining unchanged.

Figure 5 shows the experimental and calculated dependences of the excess of the averaged divergence of laser radiation (at the 85% power level) over the diffraction limit on ν_{AOS}. In the computational simulation of the AOS operation, the dynamics of the turbulent wavefront was reconstructed from a series of hartmannograms recorded in the experiment with a frequency of 1.5 kHz using the sampling scheme proposed by Fried [11]. The phase correction calculations took into account the time delay between the registration of the wavefront and the setting of the AM. It was also assumed that the AM perfectly reproduces the measured wavefront. It is seen that the calculation results are in qualitative agreement with the experimental data. Some quantitative discrepancy at high ν appears because the calculations assumed the ideal spatial resolution of the AM and at low ν it is explained by the fact that the subtraction of the background on the camera screen in the far field in experiments is accompanied by some loss of high-angle signal components.

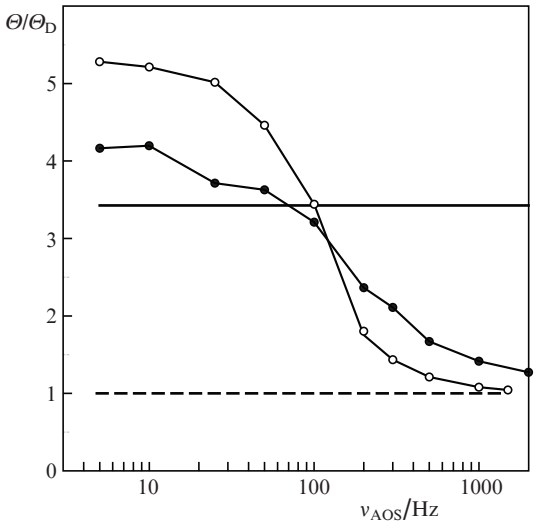

Figure 5. Dependence of the excess of the average laser radiation divergence Θ over the diffraction limit Θ_D on the AOS frequency (•) in the experiment and (○) in the calculation. The solid horizontal line is the level of the initial divergence of the laser radiation; the dashed line is the diffraction limit.

As follows from Fig. 5, when the AOS operates with a finite bandwidth, the phase correction is somehow imperfect. In our case of the Kolmogorov spectrum of centroid fluctuations, the correction is highly efficient when ν_{AOS} exceeds ν_{turb} by more than an order of magnitude: for $\nu_{turb} = 60$ Hz, this takes place at $\nu_{AOS} \geqslant 1$ kHz. With decreasing AOS bandwidth, the correction efficiency decreases. In our case, at $\nu_{AOS} \leqslant 100$ Hz, the efficiency is not just low, but 'negative', i.e., the operation of the AOS introduces additional distortions into the laser beam, the divergence of which even increases relative to the initial level.

Thus, an AOS was fabricated using a FPGA as the main control element, an AOS operating frequency of 2 kHz was achieved, a near-to-ideal dynamic correction of turbulent phase distortions lying in a frequency band characteristic of the atmosphere was demonstrated, and an experimental criterion for choosing the required AOS frequency under specific turbulence conditions was determined. In the future, we intend to submit to the 'Quantum Electronics' journal a detailed article thoroughly describing the joint experiments carried out by the authors.

Acknowledgements. This work was supported by the Russian Science Foundation (Project No. 19-19-00706).

References

1. Tan X., Wu Z., Liang Z. *Proc. SPIE*, **7284**, 72840G (2009).
2. Lu M., Bagheri M., James A.P., Phung T. *IEEE Access*, **6**, 29865 (2018).
3. Bennet F., Conan R., et al. *Proc. SPIE*, **8447**, 844744 (2012).
4. Huang Q., Liu D., Chen Y., et al. *Opt. Express*, **26**, 13536 (2018).
5. Andrews L.C., Phillips R.L. *Laser Beam Propagation Through Random Media* (Bellingham, WA: SPIE Press, 2005).
6. Rukosuev A.L., Kudryashov A.V., Lylova A.N., Samarkin V.V., Sheldakova Yu.V. *Atmosph. Ocean. Opt.*, **28**, 381 (2015).
7. Kudryashov A., Rukosuev A., Samarkin V., et al. *Proc. SPIE*, **10772**, 107720V (2018).
8. https://kayacameras.com/product-category/jetcam-high-speed-cameras/.
9. Fried D.L. *Radio Sci.*, **10**, 71 (1975).
10. Tatarski V.I. *Wave Propagation in a Turbulent Medium* (New York: McGraw-Hill, 1961; Moscow: Nauka, 1967).
11. Fried D.L. *J. Opt. Soc. Am.*, **67**, 370 (1977).